

Preparation and characterization of ambazone salt with nicotinic acid

I. Kacsó, M. Muresan-Pop, Gh. Borodi, and I. Bratu

Citation: [AIP Conference Proceedings](#) **1425**, 30 (2012); doi: 10.1063/1.3681959

View online: <http://dx.doi.org/10.1063/1.3681959>

View Table of Contents: <http://scitation.aip.org/content/aip/proceeding/aipcp/1425?ver=pdfcov>

Published by the [AIP Publishing](#)

Articles you may be interested in

[Growth and characterization of nonlinear optical single crystal: Nicotinic L-tartaric](#)

AIP Conf. Proc. **1665**, 100003 (2015); 10.1063/1.4918031

[Preparation and characterization of urea-oxalic acid solid form](#)

AIP Conf. Proc. **1425**, 35 (2012); 10.1063/1.3681960

[A solid form of ambazone with lactic acid](#)

AIP Conf. Proc. **1425**, 9 (2012); 10.1063/1.3681954

[Preparation of high-T_c superconducting oxides through a decomposition of citric acid salt](#)

AIP Conf. Proc. **219**, 355 (1991); 10.1063/1.40228

[Phosphorescence of Phenylcarboxylic Acids and Their Salts](#)

J. Chem. Phys. **52**, 3399 (1970); 10.1063/1.1673502

Preparation And Characterization Of Ambazone Salt With Nicotinic Acid

I. Kacsó¹, M. Muresan-Pop², Gh. Borodi¹, I. Bratu¹

¹National Institute for Research and Development of Isotopic and Molecular Technologies, 65-103 Donath street, 400293 Cluj-Napoca, Romania

²"Babes-Bolyai" University, Faculty of Physics, 1 Kogalniceanu Street, Cluj-Napoca, Romania

Abstract. Salt formation is a good method of increasing solubility, dissolution rate and consequently the bioavailability of poor soluble acidic or basic drugs. The aim of this study was to obtain and to investigate the structural properties of the compound that was obtained by solvent drop grinding method at room temperature starting from the 1:1 molar ratios of ambazone (AMB) and nicotinic acid (NA). The obtained compound (AMB•NA) was investigated by thermal analysis (DSC, TG-DTA), X-ray powder diffraction (PXRD) and infrared spectroscopy (FTIR). The difference between the patterns of AMB•NA and of the starting compounds evidenced the formation of a salt. Using X-ray powder diffraction data, the lattice parameters were determined. The thermal and FTIR measurements on the pure compounds and on the (1:1) grinding mixture of AMB with NA confirm the salt formation.

Keywords: ambazone nicotinate salt, powder X-ray diffraction, FTIR, thermal analysis.

PACS: 61.05.cp, 61.66.Hq, 81.70. Pg, 82.80.Gk

INTRODUCTION

Traditionally, the solid form selection process was limited to the free drug or pharmaceutically accepted salts [1]. Polymorphs, co crystals, solvates or salts, exhibit different properties compared with free drugs and can now significantly increase the options for the development of different solid forms. The salts differ from other solid forms in the following way: in salts, a proton is transferred from the acidic to the basic functionality of the crystallization partner, as the *pKa* difference between the partners is sufficiently large [1, 2].

The solid form influences relevant physical-chemical parameters such as solubility, dissolution rate of the drug, chemical stability, melting point, and hygroscopic parameter which can result in solids with superior properties. The bioavailability is strongly influenced by the solubility and the dissolution profile, these can have significant consequences and determine if the compound is further developed.

Ambazone monohydrate, $C_8H_{11}N_7S \cdot H_2O$ ([4-(2-(Diaminomethylidene)hydrazinyl)phenyl]iminothio urea], (AMB, Fig. 1.a.) one of the oldest antimicrobial chemicals is a microcrystalline powder with a very slight solubility in water and in the other organic solvents, having the melting point around 192-194°C with decomposition. Ambazone undergoes three protonation reactions with *pK* values at 10.69 (equilibrium between the negatively charged and neutral forms), 7.39 (equilibrium between the neutral and singly positively charged form) and 6.22

(equilibrium between the singly and doubly positively charged form) [3]. Recently, the antineoplasm properties of AMB were also demonstrated [8] and that accelerated the researches on this substance, without mutagenic effects and unpleasant reactions characteristic to other oncostatic drugs.

Nicotinic acid, $C_6H_5NO_2$ (also known as vitamin B₃, Niacin and vitamin PP) (NA, Fig. 1.b.) is one of the essential human nutrients. This colorless, water-soluble solid is a derivative of pyridine, with a carboxyl group (-COOH) at the 3-position. It is a weak-electrolyte, with *pKa* values of 4.9 for the aromatic ring N and approx. 2.1 for the COOH group [9]. Nicotinic acid is used as vasodilating medicines and in the treatment of diseases of the gastroenteric tract [10].

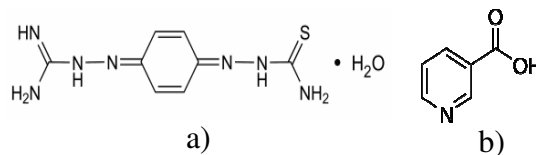


FIGURE 1. Ambazone monohydrate (a) and nicotinic acid (b) molecules.

There are many methods by which solid forms may be prepared, mostly common being solution-based crystallization and grinding. Mechanical chemical method [11–13], more commonly and usefully described as grinding, has been employed extensively in the preparation of solid forms. The range of grinding conditions has been extended by the addition

of solvents in the “solvent-drop” method [13, 14] and this may represent the introduction of solution conditions on a limited scale to the grinding process. The obtained solid form was characterized by several physical methods such as X-ray powder diffraction, FTIR spectroscopy and thermal analysis. The employed methods demonstrate the formation of the ambazone nicotinate salt.

MATERIALS AND METHODS

Ambazone was obtained from *Microsin SRL* Bucharest, Romania, the nicotinic acid from *Sigma*, Germany and both compounds were used without further purification.

The ambazone nicotinate (AMB•NA) was prepared using the so-called “solvent-drop” grinding (SDG) method, by grinding a mixture of 255.3 mg AMB and 123.11 mg NA with 1 ml twice distilled water added in drops in an agate mortar at room temperature, until a dried compound was obtained.

X-ray Powder Diffraction

X-ray powder diffraction patterns were obtained using Bruker D8 Advance diffractometer, sealed Cu tube $k = 1.5406 \text{ \AA}$ equipped with an incident beam Ge 111 monochromator.

FTIR Spectroscopy

FTIR spectra were obtained with a JASCO 6100 FTIR spectrometer in the 4000 to 400 cm^{-1} spectral domain with a resolution of 4 cm^{-1} using KB pellet technique.

Thermal Analysis

Differential scanning calorimetry (DSC) was carried out by means of a Shimadzu DSC-60 calorimeter. The sample was heated in the range of 30 – 350°C with a heating rate of $10^\circ\text{C}/\text{min}$ in crimped aluminum sample cell. The purge gas was nitrogen at $60 \text{ ml}/\text{min}$. For data collection and analysis the TA-WS60 and TA60 2.1 Shimadzu software were employed.

Differential thermal analysis (DTA) and thermogravimetry (TG) were obtained with a Simultaneous Thermogravimetric and Differential Thermal Analyzer of Shimadzu type DTG-60/60H. The measurements were performed by using alumina cells. The sample was heated in the range 30 – 350°C with a rate of $10^\circ\text{C}/\text{min}$ in alumina sample cell under dry nitrogen purge ($70 \text{ ml}/\text{min}$).

RESULTS AND DISCUSSIONS

X-ray Powder Diffraction

Figure 2 shows the XRD patterns for AMB, NA and their salt obtained by SDG method.

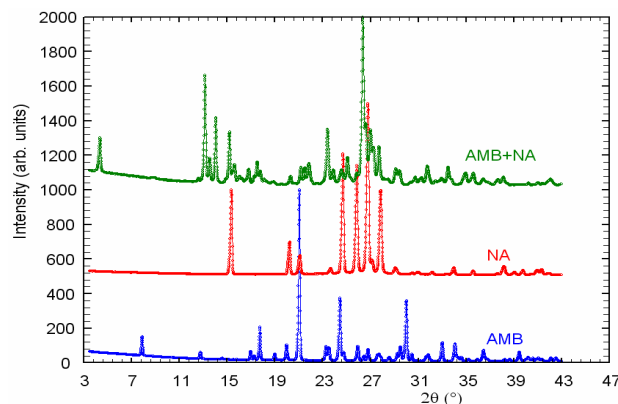


FIGURE 2. XRD patterns of AMB, NA and their salt obtained by SDG method.

The XRD pattern of AMB•NA is different as compared to those of AMB and NA ones. So, a new crystalline compound was obtained, which belongs to the monoclinic system and has the following unit cell parameters: $a=7.422 \text{ \AA}$, $b=40.439 \text{ \AA}$, $c=6.905 \text{ \AA}$, $\alpha=90^\circ$, $\beta=106.43^\circ$, $\gamma=90^\circ$.

FTIR Spectroscopy

The characteristic peaks of nicotinic acid can be recognized in the pure Nicotinic acid spectrum as to be: $\nu(\text{O-H})$ 3581 cm^{-1} , $\nu(\text{C-H})$ 3074 cm^{-1} , $\nu(\text{C=O})$ 1716 cm^{-1} , $\nu(\text{C=C})$ 1595 – 1416 cm^{-1} , $\delta(\text{C-H})$ (in-plane) 1183 – 1039 cm^{-1} [19].

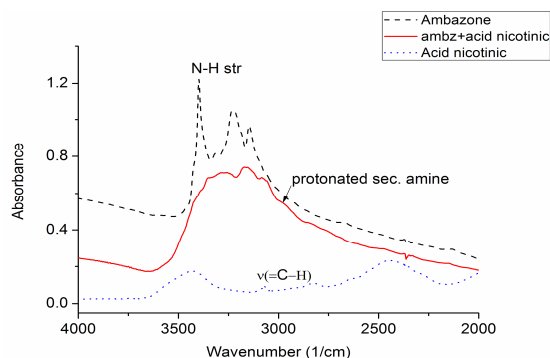


FIGURE 3. FTIR spectra of AMB, NA and AMB•NA, 4000 – 2000 cm^{-1} spectral region.

The band at $\sim 3400\text{ cm}^{-1}$ can be assigned to N–H stretching of primary amine in pure ambazone (see Fig. 3); it can be also observed as a shoulder in the spectrum of AMB•NA.

In the case of pure AMB, the FTIR spectrum contains two NH_2 vibrations (3300 and 3500 cm^{-1}) [15, 16] and NH ($3320\text{--}3180\text{ cm}^{-1}$, i.e., 3226 cm^{-1}) [16, 17]. The salt formation has been shown to modify the NH stretching absorption in amines [16, 18]; it was observed that the free bases have a sharp strong band at $\sim 3226\text{ cm}^{-1}$ due to the NH stretching and that this band is greatly reduced in intensity in the spectra of the AMB•NA. The band at 3146 cm^{-1} corresponds to the NH vibration [16] for pure AMB. The band at 3164 cm^{-1} can be assigned to N–H stretching of secondary amine in salt spectrum. A new shoulder appeared at $\sim 2970\text{ cm}^{-1}$ probably due to the protonated secondary amine [16].

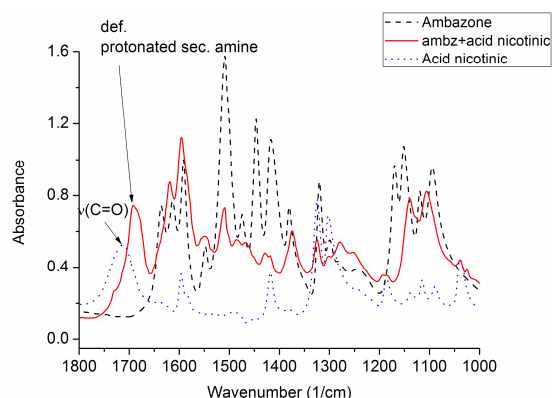


FIGURE 4. FTIR spectra of AMB, NA and AMB•NA, 1800–900 cm^{-1} spectral region

Primary amine has an absorption band of medium intensity at $\sim 1613\text{ cm}^{-1}$ (see Fig. 4), being located at $\sim 1618\text{ cm}^{-1}$ by salt formation [17]. Cleaves and Phylar [18] correlated the spectral bands at $1625\text{--}1516\text{ cm}^{-1}$ with NH deformation vibration. Pure ambazone spectrum contains the secondary amine vibration at 1508 cm^{-1} which is not shifted in AMB•NA spectrum. In the spectrum of the salt a new strong absorption appeared at $\sim 1692\text{ cm}^{-1}$, which is assigned to deformation vibration of the protonated secondary amino group (Fig.4) [20]. This frequency is not present in the FTIR spectrum of pure AMB, i.e., a salt was formed between ambazone and nicotinic acid.

Thermal Analysis

DSC

The DSC curves of the pure AMB and of the compound obtained by solvent-drop grinding (SDG) between AMB and NA are presented in Fig. 5. The curve for the pure AMB revealed a broad endothermic signal from 109 to 140°C , with a maximum at 125°C and $\Delta H=4.8\text{ kJ/mol}$, that corresponds to the water loss, followed by a sharp exothermic signal at 204°C with $\Delta H=126\text{ kJ/mol}$, due to the melting with decomposition of AMB.

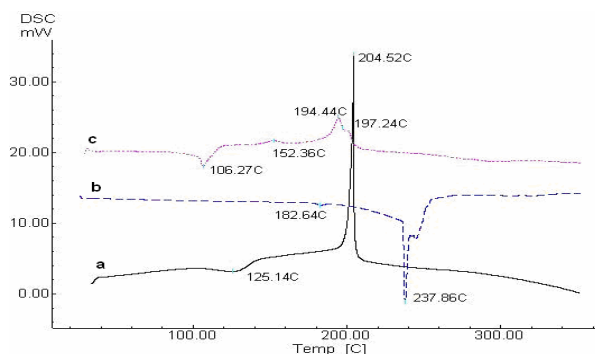


FIGURE 5. DSC of AMB (a), NA (b) and AMB•NA (c) obtained by SDG.

The thermal behavior of nicotinic acid presents an endothermic peak between $180\text{--}185^\circ\text{C}$, $\Delta H=1.66\text{ kJ/mol}$, due probably to solid-solid transition. Another sharp endotherm is observed between $236\text{--}239^\circ\text{C}$, $\Delta H=27.92\text{ kJ/mol}$, corresponding to the melting of the sample, followed by a small endothermic peak between $242\text{--}270^\circ\text{C}$ due to the sublimation of the nicotinic acid [20].

The DSC curve of AMB•NA presents four events: an endothermic peak between 80 and 115°C , with $\Delta H=32.37\text{ kJ/mol}$, corresponding to the loss of water molecules, an exothermic peak between 142 and 158°C , $\Delta H=11\text{ kJ/mol}$, due probably to the solid-solid transition, an exothermic peak between 190 and 197°C with $\Delta H=31.61\text{ kJ/mol}$, followed by another exotherm between $198\text{--}204^\circ\text{C}$, $\Delta H=6.44\text{ kJ/mol}$, corresponding to the melting with decomposition of the sample.

DTA-TG

The simultaneous DTA–TG measurements of the AMB revealed the thermal behavior of this compound (Fig. 6).

TG–DTA traces of AMB show thermal stability up to 85°C . Between 86°C and 149°C the first mass loss occurs (6.85%) corresponding to a broad endothermic

peak between 100 and 140°C with maximum at 122°C. Next mass loss, 26.05%, occurs in the range 185–220°C and corresponds to a sharp exotherm on the DTA curve between 180 and 225°C with peak maximum around 209°C. This signal corresponds to the mass loss of the volatile components resulted from the AMB decomposition.

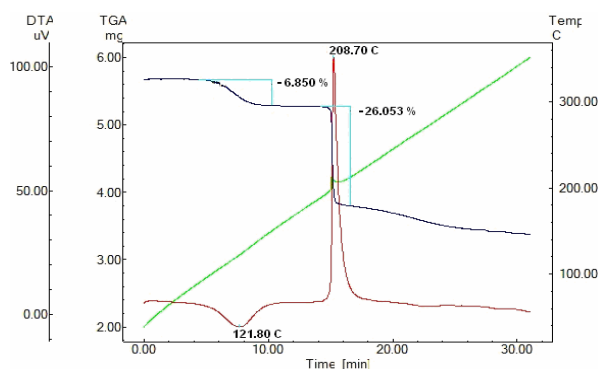


FIGURE 6. DTA–TG of AMB.

The obtained data present a very good similarity with DSC measurements.

The DTA–TG measurements of the AMB•NA revealed the thermal behavior of the compound obtained by SDG method (Fig. 7).

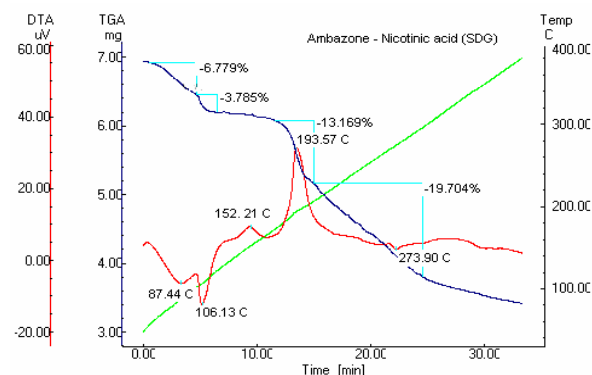


FIGURE 7. DTA–TG of AMB•NA obtained by SDG.

TG–DTA traces of AMB•NA indicate in the 60–100°C temperature range the first mass loss of 6.78%, corresponding to a broad endothermic peak and another endotherm between 100 and 130°C with maximum at 106°C and mass loss of 3.78% due to the non-bonded and bonded water elimination. The third mass loss of 13.17% occurs between 180 and 210°C, probably due to nicotinic acid sublimation and evaporation. This step of mass loss corresponds to a sharp exotherm with T_{onset} at 175°C and peak maximum at 193.5°C. In the 210–350°C range, the

final mass loss of 19.70% occurs, corresponding to the elimination of volatile components resulting from decomposition of ambazone and evaporation of the nicotinic acid. These signals have good similarity with DSC measurements.

CONCLUSIONS

Based on X-ray powder diffraction and DTA–TG–DSC data we conclude that, starting from ambazone and nicotinic acid and using the SDG preparation method, a new crystalline compound was formed.

FTIR data indicate the AMB•NA salt formation by the appearance of the frequencies characteristic to NH_2^+ group.

ACKNOWLEDGMENTS

The FTIR, powder X-ray diffraction and DSC, TG–DTA measurements were supported by the PN 09-44 02 01/2009 and PN 09-44 02 05/2009 projects.

REFERENCES

1. H. G. Brittain, *Polymorphism in pharmaceutical solids. Drugs and the pharmaceutical sciences*. 2nd ed., vol. 192. New York: Informa Healthcare; 2009.
2. <http://www.pharmaceutical-int.com/categories/cocrystalsco-crystals-an-attractive-alternative-for-solid-forms.asp>. 2007.
3. G. Löber and H. Hoffmann, *Biophys Chem* **35**, 287–300 (1990).
4. I. Fichtner and W. Arnold, *Pharmazie* **38**, 130–131 (1983).
5. H. J. Kuhnel, R. Amlacher, K. Kramarczyk and W. Schulze, *Pharmazie* **43**, 197–199 (1988).
7. J. Baumgart, N. V. Zhukovskaya and V.N. Anisimov, *Exp Pathol*. **33**, 239–248 (1988).
8. W. Gutsche, A. Hartl, J. Baumgart and W. Schulze, *Pharmazie* **45**, 55–57 (1990).
9. K.Y. Tim and K. Takacs-Novak, *Pharm. Res.* **16**, 377–381 (1999).
10. E. N. Makareyer, Y. V. Makedonov and E. L. Lozorskaya, *Russ Chem Bull*, **46** (1997).
11. M. C. Etter and D. A. Adsmond, *J Chem Soc Chem Commun*. **8**, 589–591 (1990).
12. M. Otsuka, K. Otsuka and N. Kaneniwa. *Drug Dev Ind Pharm*. **20**, 1649–1660 (1994).
13. N. Shan, F. Toda and W. Jones, *Chem Commun(Camb.)* **20**, 2372–2373 (2002).
14. A. V. Trask, W. D. S. Motherwell and W. Jones, *Chem Commun (Camb.)* **7**, 890–891 (2004).
15. B. B. Koleva, T. Kolev, R. W. Seidel, M. Spiteller, H. Mayer-Figge and W. S. Sheldrick, *J Phys Chem A*. **113**, 3088–3095 (2009).
16. R. Heacock and L. Marion, *Can J Chem*. **34**, 1782–1795 (1956).

17. G. Socrates, *Infrared and Raman characteristic group frequencies: tables and charts*. 3rd ed Wiley, West Sussex; 2001. pp. 332.
18. A. P. Cleaves and E.K. Plyler, *J Chem Phys.* **7**, 563-569 (1939).
19. S. Jingyan, L. Jie, D. Yun, H. Ling, Y. Xi, W. Zhiyong, L. Yuwen and W. Cunxin, *J. Therm Anal Calorim*, **93**, 403-409 (2008).
20. M. Muresan-Pop, I. Kacso, C. Tripon, Z. Moldovan, Gh. Borodi, S. Simon, I. Bratu, *J. Therm Anal Calorim* **104**, 299-306 (2011).